App. Envi. Res. 39(2) (2017): 77-87

Applied Environmental Research

Journal homepage : http://www.tci-thaijo.org/index.php/aer

A GIS Model for PM_{10} Exposure from Biomass Burning in the North of Thailand

Borworn Mitmark[1], Wanida Jinsart[2,*]

[1] Interdepartment of Environmental Science, Graduate School, Chulalongkorn University, Bangkok, Thailand
[2] Department of Environmental Science, Faculty of Science, Chulalongkorn University, Bangkok, Thailand
[*] Corresponding author: Email: jwanida@chula.ac.th

Article History
Submitted: 21 February 2017/ Accepted: 10 April 2017/ Published online: 21 July 2017

Abstract

Human exposure to particulate matter with an aerodynamic diameter below 10 µm (PM_{10}) is found to be associated with biomass burning in Thailand. Recent investigations confirm that primary sources of PM_{10} are natural forest fires and agricultural waste burning. Incidence of atmospheric haze increases significantly during the dry season from January to April. PM_{10} exposure in eight provinces in Northern Thailand were determined using GIS through spatial interpolation. Daily average ambient PM_{10} concentrations from 10 monitoring stations were used as the input data for the GIS model. Three interpolation techniques: Inverse Distance Weighted (IDW), Kriging and Spline, were compared. The predicted PM_{10} concentrations were verified with field measurements. GIS-based maps illustrated the variability of PM_{10} distribution and high-risk locations, which were found to be associated with wind direction and forest fire frequencies. Mae Hong Son, Chiang Rai and Phrae were found to be at highest risk of PM_{10} exposure during the dry season.

Keywords: GIS; PM_{10} exposure; Haze; Biomass burning

Introduction

Recently, Geographic Information Systems (GIS) have been widely employed as a tool for environmental quality assessment. For example, it has been used as a tool to map wildfire risk in several regions to define hotspots for environmental risk [1]. Managers and planners are increasingly using GIS-based models to assess the performance of air quality monitoring networks in urban areas [2]. The application of GIS in epidemiology has also increased, particularly to assess human exposure [3]. Quantitative health risk assessments are normally based on comparisons of exposure concentrations against

toxic reference doses or to mandated regulatory values. An exposure level can be assessed by either direct measurement or by prediction from mathematical models using various matrices and exposure scenarios [4]. Despite its high cost, direct measurement is generally preferred as it allows exposure and concentrations to be quantified. However, exposure assessment for atmospheric pollution from wild fires can be performed using alternative approaches such as satellite imagery [5], remote sensing to measure aerosol optical thickness [6], estimated emissions using Moderate Resolution Imaging Spectro-radiometer (MODIS) [7] and mapping of risk area from wildfires by GIS interpolation [8].

In this study, PM_{10} distribution and risk areas were mapped to compare two events, with and without biomass burning in Northern Thailand. Spatial analysis was used to estimate PM_{10} exposure and identify vulnerable areas. Spatial analysis of PM_{10} concentrations was carried out by interpolation of data obtained from an ambient air monitoring station, using different interpolation methods.

Study area and data resources

1) Site selection and monitoring stations

The topography of Northern Thailand comprises different variations of valleys surrounded by paddy fields, sandwiched between mountain ranges. Eight provinces, namely Chiang Mai, Chiang Rai, Lamphun, Lampang, Phrae, Nan, Phayao and Mae Hong Son were selected as the study sites. The combined population of these provinces is approximately 5,853,206 [9]. The provincial boundaries and 10 air quality monitoring stations (Figure 1) are adapted from the work of Pungkhom and Jinsart, 2014 [8]. The coordinates of the monitoring stations are summarized in Table 1.

2) Data analysis

Data of the average daily PM_{10} concentrations from 2011 to 2015 were obtained from the Pollution Control Department (PCD). Atmospheric conditions, wind speed and wind direction were obtained from the Thai Meteorological Department (TMD). Data on the frequency of forest fires were obtained from the Forest Fire Control Division, Royal Forest Department (FFCD). Agricultural land use data from 2008-2015 were provided by the Land Development Department (LDD).

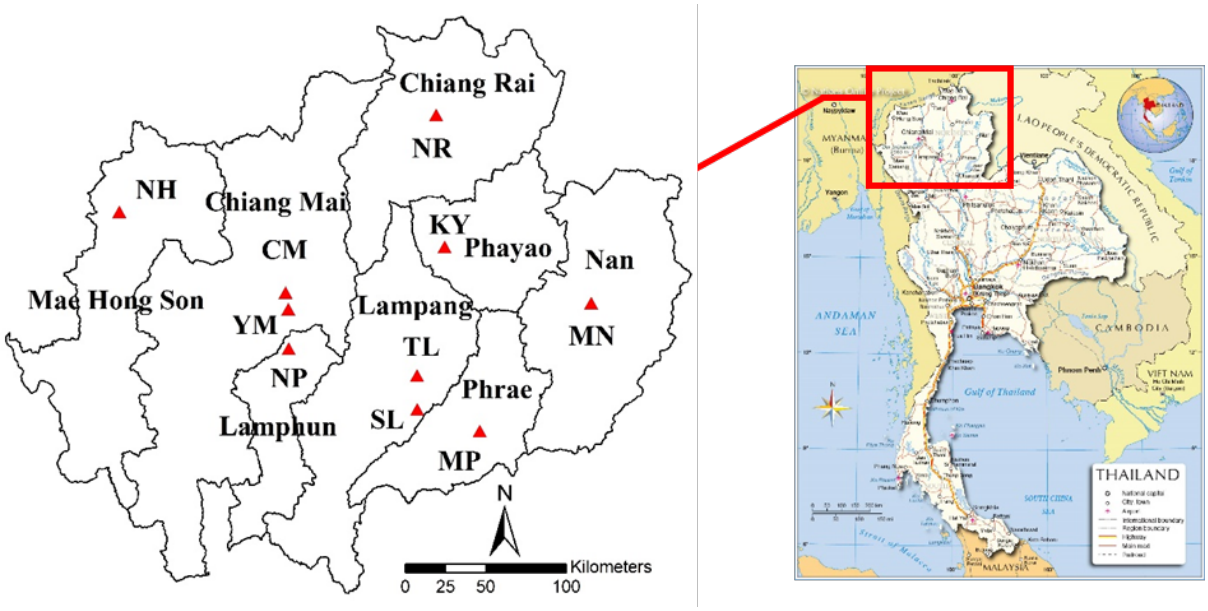

Figure 1 Study area and location of monitoring stations.

Table1 Study sites and monitoring stations coordinate X, Y position in UTM

Province	Monitoring Station	UTM ZONE 47 N	
		X	Y
Lampang	Sob Pad (SL)	580762	2018151
	Ta See (TL)	579879	2039236
Chiang Mai	City Hall Chiang Mai (CM)	496709	2088015
	YupparajWittayalai School (YM)	498803	2077766
Chiang Rai	Natural Resources and Environment Office Chiang Rai (NR)	586166	2201696
Mae Hong Son	Natural Resources and Environment Office Mae Hong Son (NH)	392292	2134528
Lamphun	Main Stadium of Lamphun (NP)	499848	2053317
Phayao	Knowledge Park Phayao (KY)	594257	2119842
Phrae	Meteorological Phrae (MP)	619922	2005915
Nan	Muang Nan Municipality Office (MN)	686341	2087939

GIS interpolation and its verification

Spatial interpolation of PM_{10} concentration measured from 10 ambient air quality monitoring stations in the study area was carried out using ArcGIS10.1. Three interpolation schemes, i.e. inverse distance weighted (IDW), kriging and spline were compared and verified against the measurement values at the test point. The IDW, kriging and spline model were calculated by the different approaches.

1) Interpolation method

The IDW interpolation determines cell values using a linearly weighted combination of a set of sample points. The weight is a function of inverse distance, and the variable being mapped decreases in influence with distance from its sampled location. The significance of known points on the interpolated values was based on their distances from the output point [10]. For example, in the case of height calculation, the following Eq. 1 is used.

$$Zj = \frac{\sum_{i=1}^{n}\left(\frac{Z_i}{d_i^p}\right)}{\sum_{i=1}^{n}\left(\frac{1}{d_j^p}\right)} \qquad \text{(Eq. 1)}$$

In this equation, p refers to the speed reducer weight control rate obtained from the distance, which is equal to 2; d_i refers to the distance from an unknown point to a known point; and z_i represents the height of point I [11-12].

Kriging interpolation generates an estimated surface from a scattered set of points with z-values and assumes that the distance or direction between the sample points probably reflects a spatial correlation. To determine the output value for each location, the Kriging tool has a mathematical function to the specified number of points, or all points within a specified radius. Kriging is a multistep process of performing exploratory statistical analysis of the data, variogram modeling, creating the surface, and exploring a variance surface. The general equation is shown in Eq. 2.

$$\hat{Z}(s_0) = \sum_{i=1}^{N} \lambda_i Z(s_i) \qquad \text{(Eq. 2)}$$

Where $Z(s_i)$ is the measured value at the i^{th} location, λ_i is an unknown weight for the measured value at the i^{th} location, s_0 is the predicted location and N is the number of measured values [10].

The spline interpolation estimates a value by using a mathematical function to minimize overall surface curvature, resulting in a smooth surface that passes exactly through the input

points. Conceptually, the sample points should extrude to the height of their magnitude. This method bends a sheet of rubber that passes through the input points while minimizing the total curvature of the surface. It fits a mathematical function for the specified number of the nearest input point, while passing through the sample points, as shown in Eq. 3.

$$S(x,y) = T(x,y) + \sum_{j=1}^{N} \lambda_j R(r_j) \qquad \text{(Eq. 3)}$$

Where j is 1, 2, ..., N, N is the number of points, λ_j is coefficients yielded by the solution of a system of linear equations and r_j is the distance from the point (x, y) to the j^{th} point [10].

2) Interpolation model verification

The performance of the three interpolation models: IDW, Kriging and Spline was compared using cross-validation analysis and the leaving-one-cut principle [13-14]. Each of the PM_{10} average values of 10 monitoring stations were recalculated against the value from the test point. Then, the interpolated results were compared to the measured values. The performance of the interpolation techniques is expressed as the mean relative error (MRE), Eq. 4 and the root mean square error (RMSE), Eq. 5.

$$MRE = \frac{1}{n} \sum_{i=1}^{n} \left| \frac{X_1 - X_2}{X_1} \right| \qquad \text{(Eq. 4)}$$

Where X_1 is the measured concentration and X_2 is the interpolation estimated PM_{10} concentrations of the i^{th} data point and n is the sample size [15].

Root mean square error (RMSE) refers to the square root of the average squared distance of a data point from the fitted line calculated by the following Eq. 5.

$$RMSE = \sqrt{\frac{1}{n} \sum_{i=1}^{n} (Y_1 - Y_2)^2} \qquad \text{(Eq. 5)}$$

Where Y_1 and Y_2 are the measured and estimated levels of the i^{th} data point and n is the total number of data points [16].

3) GIS-based map

PM_{10} concentration distribution maps were created by the best performance interpolation model. The input parameters relied on the daily average PM_{10} concentrations from 2011 to 2015, location coordinates (UTM zone 47N), topography raster map of Northern Thailand and wind directions. The GIS maps were compared between wet/dry seasons and with/without fire events.

Results and discussion

1) Comparison of spatial interpolation methods

To evaluate the accuracy of the results from the different techniques, PM_{10} distribution maps were created and shown in Figure 2. The data from 10 monitoring stations were compared against a test point at the meteorological station in Lampang province. The cross-validation used all data points to estimate the trend. It removed each data location one at a time and predicted the associated data value [17]. This analysis was rotated for test points among all 10 monitoring stations and one point from the meteorological station in Lampang. The average results of the cross-validation of IDW, Kriging and Spline are presented in Table 2. Including MRE and RMSE calculations, IDW gave the best performance interpolation of PM_{10} values with lowest MRE and RMSE (MRE = 0.0042 μg m^{-3}, RMSE = 0.9965 μg m^{-3}) in comparison to Kriging and Spline.

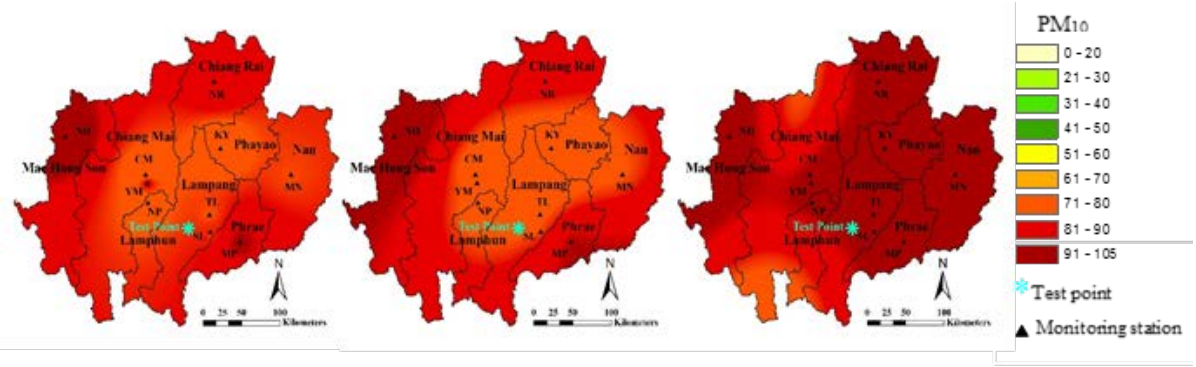

Figure 2 Comparison of three interpolation maps to the test point, coordinate in UTM, (X = 551877.38, Y = 2022215.98).

Table 2 Model performance indicators for the IDW, Kriging and Spline

Station	Measured PM_{10} ($\mu g\ m^{-3}$)	Interpolation PM_{10} ($\mu g\ m^{-3}$)		
		IDW	Kriging	Spline
SL	805.0	80.5015	80.8038	80.6242
TL	78.75	78.7516	78.8202	78.7645
CM	71.75	71.7781	73.3703	71.4081
YM	83.75	83.2384	81.6509	83.5087
NR	87.50	87.4991	87.3308	87.3562
NH	103.25	103.2480	102.8380	103.1260
NP	75.25	75.2575	75.7440	75.6207
KY	73.25	73.2504	73.4728	73.2402
MP	93.50	93.4952	93.0451	93.7430
MN	79.25	79.2502	79.4761	79.3298
Test point	83.50	80.2351	78.9979	69.9288
MRE ($\mu g\ m^{-3}$)		0.0042	0.0077	0.0168
RMSE ($\mu g\ m^{-3}$)		0.9965	1.5997	4.0966

2) PM_{10} exposure distribution maps

According to the evaluation of three interpolation models, IDW performed better than the other two models (Table 2). PM_{10} distribution maps from 2011 to 2015 data were created by IDW using ArcGIS 10.1. IDW provided a smooth surface when considering the spatial variance of data in the simulation. A raster map from spatial interpolation depicting the distribution of the PM_{10} concentrations was produced and compared as shown in GIS-based maps in Figure 3. It was found that interpolated PM_{10} concentrations increased from year 2011 to 2015 and average levels of PM_{10} were higher in dry seasons than in wet seasons. Mae Hong Son province was a dominant risk area (Figure 3a, 3c and 3e). Particularly in the year 2013, Mae Hong Son, Chiang Rai and Phrae were considered to be the high risk areas of PM_{10} exposure in the dry season (Figure 3C).

3) PM_{10} distribution and wind direction

GIS-based maps were created using IDW interpolation. The input data include average daily PM_{10} concentrations and daily wind direction from January to April 2013, representing the dry season, and data from June to October 2013, representing the wet season. Samples were collected from a total of ten sampling points (Figure 4). In Figure 4, the arrows represent the wind direction and PM_{10} concentrations are illustrated in color scale. In the dry season, high PM_{10} concentrations were found in Mae Hong Son, Chiang Rai and Phrae (Figure 4a), with

lower concentrations in the wet season (Figure 4b). Nevertheless, the distribution was not directly influenced by the wind direction because of the influence of their valley topography. An instance of a wind rising from Mae Hong Son Meteorological station is shown in Figure 4c and 4d. This indicates the main wind direction from the south. Average wind speed in the dry season (8.75 knot, gentle breeze) was higher than that in the wet season (3.23 knots, light air). It is noted that low wind speed results in poor dispersion of pollutants, leading to higher local concentration of pollutants; meanwhile, strong or turbulent winds are effective in causing rapid dispersal. However, in this area, wind speed and direction did not show significant differences. Hence, these parameters may have less effect than emission concentrations from the sources.

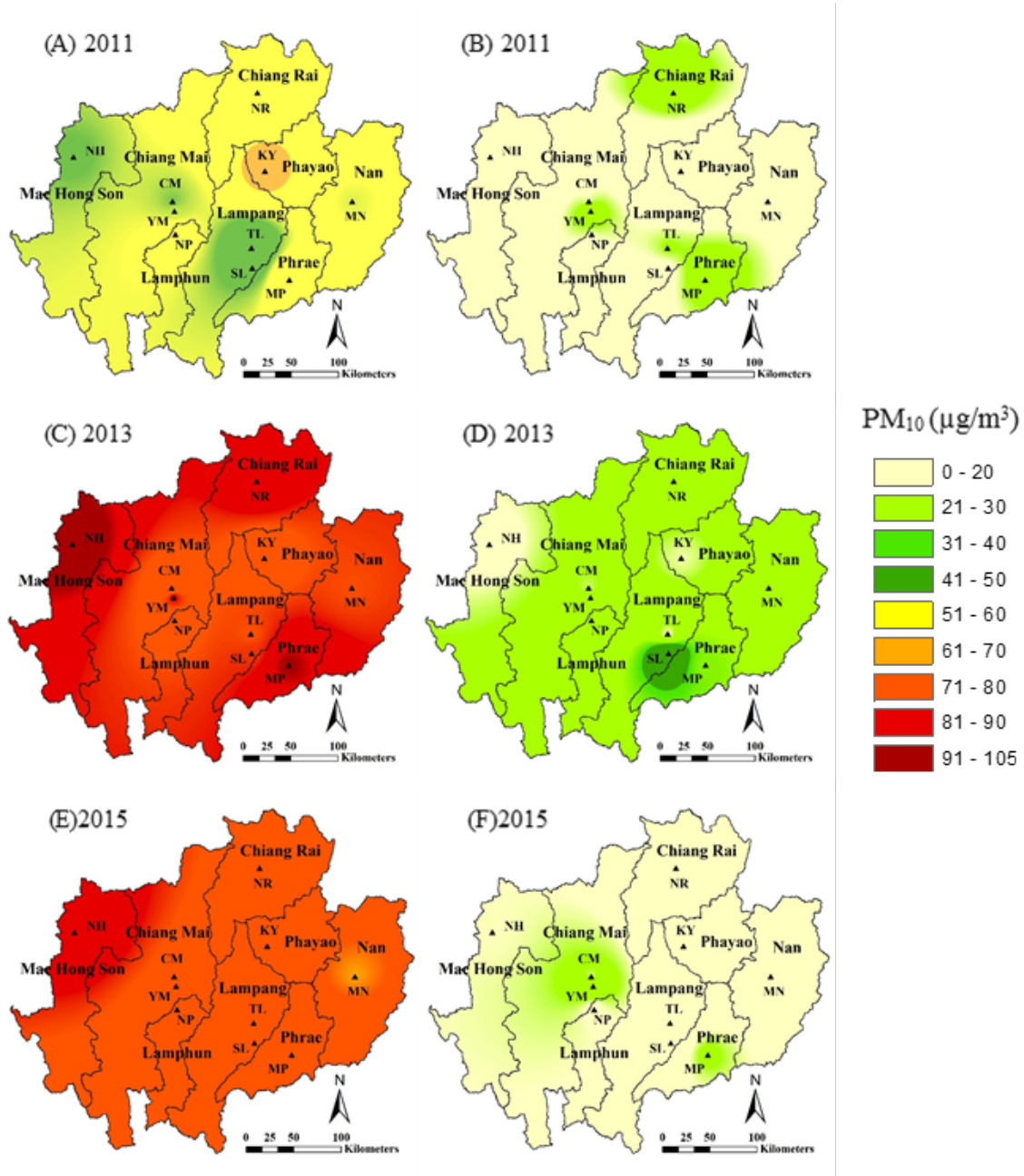

Figure 3 GIS-based map of PM_{10} concentrations in Northern Thailand (a) 2011 dry season, (b) 2011 wet season, (c) 2013 dry season, (d) 2013 wet season, (e) 2015 dry season, (f) 2015 wet season.

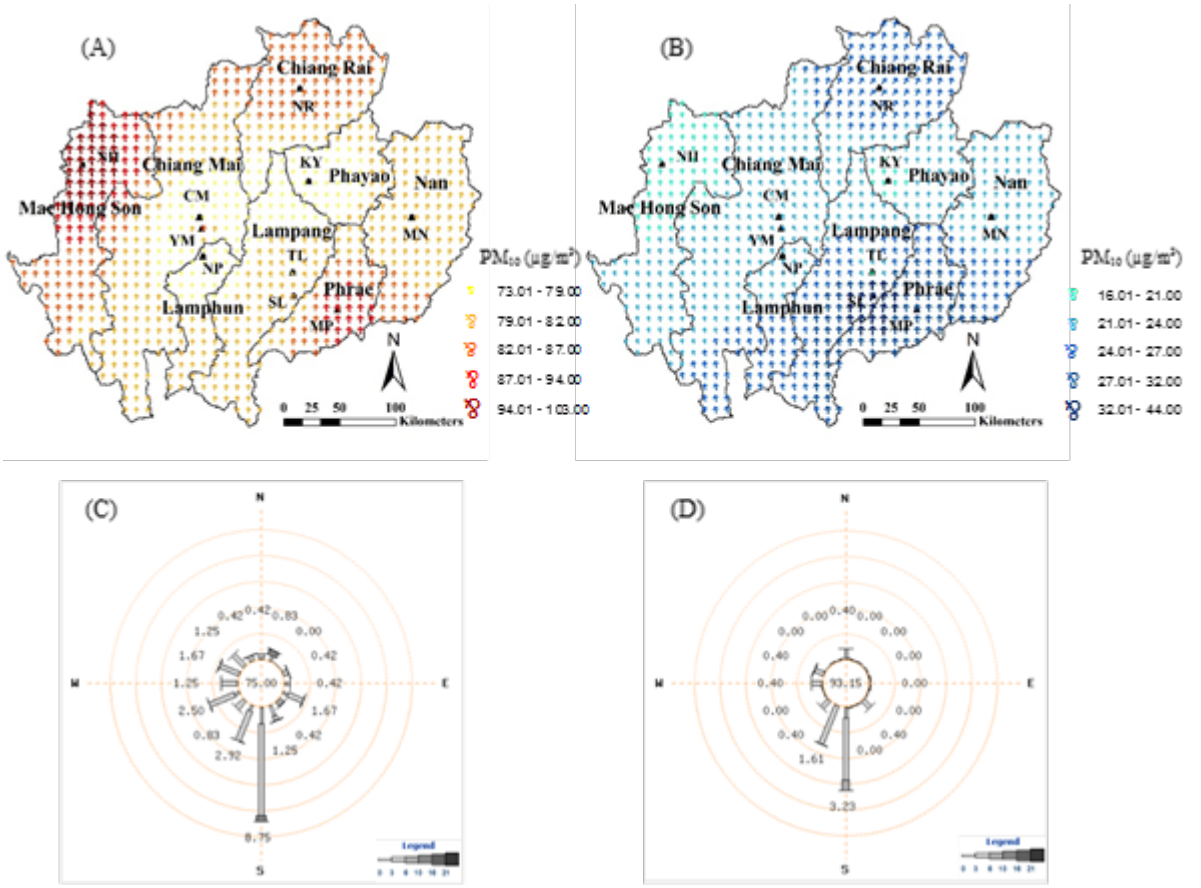

Figure 4 Map of PM_{10} distribution and wind direction in Northern Thailand (a) PM_{10} average from January-April 2013 dry season, (b) PM_{10} average from June-October 2013 wet season (c) wind rose in April 2013 dry season, and (d) wind rose in July 2013 wet season.

4) PM_{10} exposure, season variation and frequency of wildfire

The spatial daily PM_{10} concentrations of the eight provinces were compared in the dry season (January-April), wet season (July-October) and over the whole year (January-December). In Figure 5, the annual average PM_{10} concentrations at each site did not exceed the ambient PM_{10} annual standard (50 µg m^{-3}, http://www.pcd.go.th/info_serv/reg_std_airsnd01.html.) However, PM_{10} concentrations in each province were found to exceed than the ambient air quality standard during the dry season. The increased PM_{10} concentrations from 2011 to 2015 (Figure 5) were associated with increasing frequency of forest fires (Table 3). According to the Forest Fire Control Division of the Royal Forest Department (FFCD), forest fires are most frequent each year during the dry season from December to May. The frequency and extent of bushfires from 2011 to 2015 have both progressively increased each year, particularly in the far north of the country. The information of the number of fires was provided by FFCD [18]. Average PM_{10} concentrations from the eight provinces and the number of fires reported in the areas were compared (Figure 6). The highest emission levels occurred from January to April during the dry season. There is a strong correlation between ambient PM_{10} concentration and fire frequency, $r = 0.91$ ($p < 0.05$).

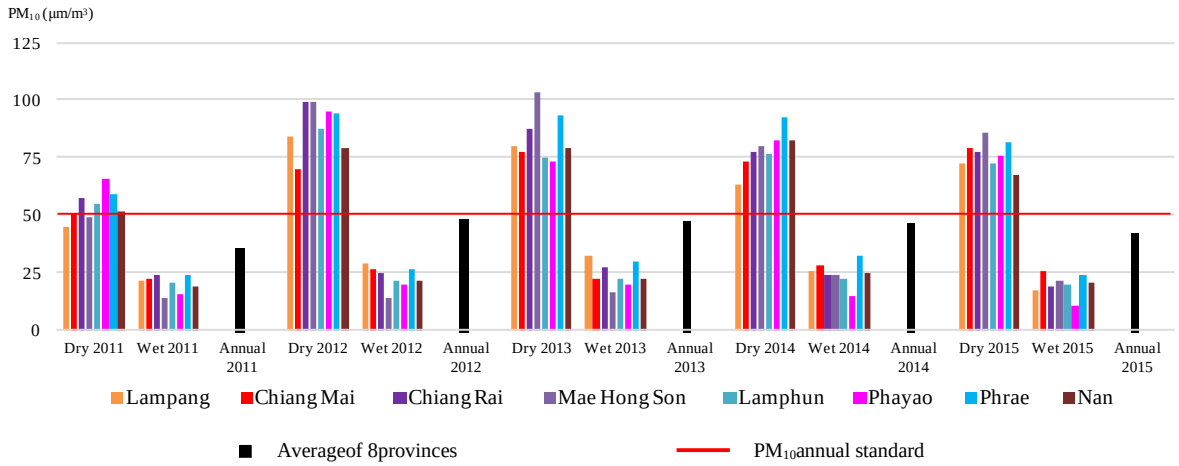

Figure 5 Comparison of average PM_{10} concentrations in 2011 to 2015 dry season (January - April), wet season (July - October) and January-December.

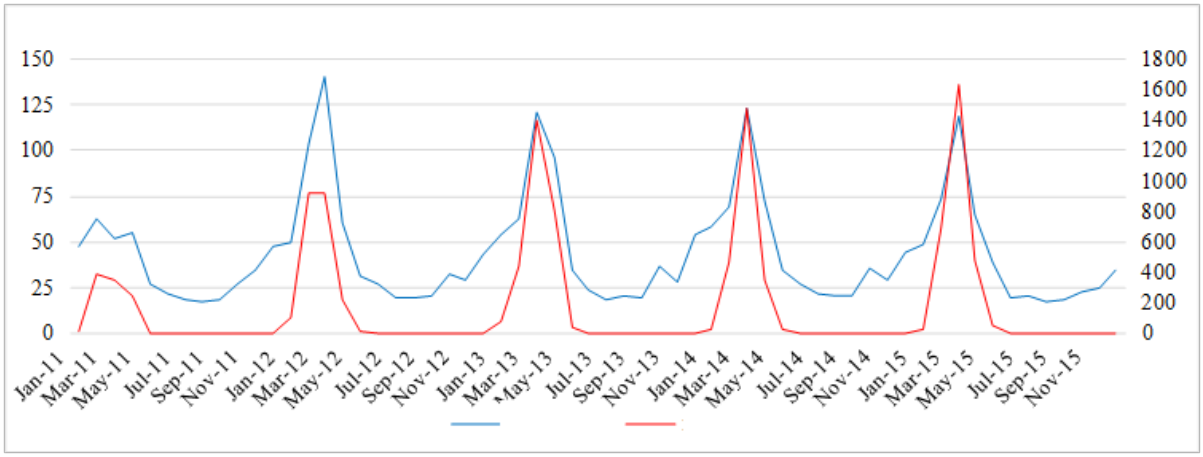

Figure 6 Temporal variation of PM_{10} and frequency of occurrence of wild fires from 2011 to 2015.

5) PM_{10} exposure and land use

In addition to the alarming increase in incidences of forest fire in the area, intensive agriculture could also influence PM_{10} levels. Burning of stubble and other crop residues/ agricultural waste to prepare the land for planting could also substantially increase PM_{10} emission. Cultivated areas in the eight provinces steadily increased during 2008-2015 (Table 3). Among the eight provinces compared, the high farm land in Chiang Rai was related to high PM_{10} concentration map in Figure 3. Chiang Rai has the highest area of agricultural land (5,682.95 km^2), accounting for about 49 % of the province's total area. IN Chiang Rai, the agricultural area in Chiang Rai was three times higher than in Phayao, which had 2,542.67 km^2 of agricultural land, occupying about 40 % of the province's total area, but only increasing by 253.50 km^2 over the period 2008-2015. This province was not yet at risk. Phrae's agricultural area was 2,585.70 km^2, with an increase of 1,160.29 km^2 over the 2008 area. The GIS map confired that Chiang Rai and Phrae were at high risk of PM_{10} exposure. On the other hand, in Mae Hong Son Province, while the agricultural area increased by only 346.57 km^2, there was a continuous increase in biomass burning in addition to pollutants emitted from across the border with Myanmar [8]. So PM_{10} exposure in Figure 3 seemed to be dominant in this province. Further monitoring and pollution prevention efforts are recommended for Mae Hong Son, Chiang Rai and Phrae Provinces, as high risk

areas. This work illustrated the application of GIS in prediction of PM_{10} exposure from wildfire pollutants, taking into account the many influencing factors. Using these methods would contribute to air quality management and biomass burning control.

Table3 Agriculture area (rai) and % compared to total province area were summarized in two groups of survey duration in 2008-2010 and 2012-2015 [19].

Land Use: Agriculture areas (1 rai = 0.4 acre)					
Province	**Years 2008-2010**		**Years 2013-2015**		**Increasing**
	Rai	**%**	**Rai**	**%**	**Rai**
Chiang Mai	2,777,253	22.02	3,004,782	23.91	227,529
Chiang Rai	3,217,613	44.07	3,551,846	48.66	334,233
Lampang	1,311,388	16.74	1,690,953	21.56	379,565
Lamphun	797,199	28.31	864,976	30.7	67,777
Mae Hong Son	1,168,741	14.76	1,385,345	17.48	216,604
Phayao	1,430,728	36.14	1,589,168	40.1	158,440
Phrae	890,881	21.79	1,616,061	28.41	725,180
Nan	1,912,265	26.67	2,420,786	33.76	508,521

Conclusions

This study presents and evaluates approaches to estimating spatial variability in ambient air pollution concentrations in Northern Thailand. Spatial interpolation of the PM_{10} concentrations measured from 10 ambient air quality monitoring stations in the study area was carried out using three separate spatial interpolation schemes. Empirical measurements used in this study included the inverse distance weighted (IDW), Kriging and Spline. The different interpolation techniques were evaluated by cross-validation at the test point, which is a standard method [17]. The findings indicated that the IDW method produced superior results compared to Kriging and Spline. However, it should be noted that the choice of method will be case-specific. For mapping of PM_{10} pollution, it is necessary to compare several integrating and interpolating techniques of the secondary data prior to applying the suitable method for further analysis. The PM_{10} concentrations of the eight provinces in the dry season were reportedly higher than in the wet season. From PM_{10} concentration map identification and average PM_{10} in 2011-2015, the three high health risk areas from PM_{10} in the north of Thailand include Mae Hong Son, Chiang Rai and Phrae Provinces.

Acknowledgements

This study was supported by Department of Environmental Quality Promotion, Ministry of Natural Resources and Environment. The authors deeply appreciate the assistance of the Pollution Control Department, Department of Forest Fire Management, Thai Meteorological Department and the Land Development Department in providing data.

References

[1] Chuvieco, E., Aguado, I., Yebra, M., Nieto, H., Salas, J., Martin, M.P. …, Zamora, R., Development of a framework for fire risk assessment using remote sensing and geographic information

system technologies. Ecological Modelling, 2010, 221, 46-58.

[2] Pope, R., Wu, J., A multi-objective assessment of an air quality monitoring network using environmental, economic and social indicators and GIS-based model. Journal of the Air & Waste Management Association, 2014, 64 (6), 721-737.

[3] Pearcea, L.J., Waller, A.L., Sarnat, E.S., Chang, H.H., Kleinc, M., Mulholland, A.J., Tolbert, E.P., Characterizing the spatial distribution of multiple pollutants and populations at risk in Atlanta, Georgia. Spatial and Spatiotemporal Epidemio-logy, 2016, 18, 13-23.

[4] Ann, W., Richard, B., Donald, K. Assessment of human exposure to air pollution: methods, measurements, and models. Air Pollution, the Automobile, and Public Health, 1988. [Online] Available from: https://www.ncbi.nlm.nih.gov/books/n/nap1033/pdf/

[5] Sirimongkonlertkula, N., Upayokhin, P., Phonekeob, V., Multi-temporal analysis of haze problem in Northern Thailand: A case study in Chiang Rai Province. Kasetsart Journal (Natural Science), 2013, 47, 768-780.

[6] Sirimongkonlertkula, N., Phonekeob, V., Remote sensing and GIS application analysis of active fire, aerosol optical thickness and estimated PM_{10} in the north of Thailand and Chiang Rai Pro-vince, APCBEE Procedia, 2012, 1, 304-308.

[7] Junpen, A., Garivait, S., Bonnet, S., Estimating emissions from forest fires in Thailand using MODIS active fire product and country specific data. Asia-Pacific Journal of Atmospheric Sciences, 2013, 49(3), 389-400.

[8] Pungkhom, P., Jinsart, W., Health risk assessment from bush fire air pollutants using statistical analysis and geographic information system: Case study in the northern Thailand. International Journal of Geoinformatics, 2014, 10(1), 17-24.

[9] DOPA-Department of Provincial Administration, population in the north of Thailand, 2016. [Online] Available from: http://stat.dopa.go.th/stat/statnew/upstat_age.php

[10] ESRI-Environmental Systems Research Institute, Raster Interpolation toolset concepts, 2016. [Online] Available from: http://desktop.arcgis.com/en/arcmap/10.3/tools/3d-analyst-toolbox/understanding-interpolation-analysis.htm

[11] Lu, Y. G., Wong, W. D., An adaptive inverse-distance weighting spatial interpolation technique. Computers and Geosciences, 2008, 34, 1044-1055.

[12] De Mesnard, L., Pollution models and inverse distance weighting: Some critical remarks. Computers and Geosciences, 2013, 52, 459-469.

[13] Janssen, S., Dumont, G., Fierens, F., Mensink, C. Spatial interpolation of air pollution measurements using CORINE land cover data. Atmospheric Environment, 2008, 42, 4884-4903.

[14] Thepanondh, S., Toruksa, W. Proximity analysis of air pollution exposure and its potential risk. Journal of Environmental Monitoring, 2011, 13, 1264-1270.

[15] Xie, Y., Chen, T., Lei, M., Yang, J., Gou, Q., Song, B., Zhou, X., Spatial distribution of soil heavy metal pollution estimated by different interpolation methods: Accuracy and uncertainty analysis. Chemosphere, 2011, 82, 468-476.

[16] Gong, G., Mattevada S., O'Bryant E S., Comparison of the accuracy of kriging and IDW interpolations in estimating groundwater arsenic concentrations in Texas. Environmental Research, 2014, 130, 59-69.

[17] ESRI-Environmental Systems Research Institute, Performing cross-validation and validation, 2016. [Online] Available from: http://desktop.arcgis.com/en/arcmap/latest/extensions/geostatistical-analyst/performing-cross-validation-and-validation.htm#GUID-7460E552-DAF6-4D04-8247-8B5866D7B06D

[18] FFCD-Forest Fire Control Division National Park, Forest fire statistics, 2015. [Online] Available from: http://www.dnp.go.th/forestfire/2546/firestatistic%20Th.htm

[19] LDD-Land Development Department, Land use data of agriculture area, 2016. [Online] Available from: http://www.ldd.go.th/web_OLP/report_research_N.html#north.